Rational design of a tunable pH-triggered DNA nanoswitch

Andrea Idili[1,2], Alexis Vallée-Bélisle[3,*], and Francesco Ricci[1,2,*]

[1] Dipartimento di Scienze e Tecnologie Chimiche, University of Rome, Tor Vergata, Via della Ricerca Scientifica, 00133, Rome, Italy, [2] Consorzio Interuniversitario Biostrutture e Biosistemi "INBB", Rome, Italy, [3] Laboratory of Biosensors and Nanomachines, Département de Chimie, Université de Montréal, Québec, Canada; *Corresponding authors: francesco.ricci@uniroma2.it; a.vallee-belisle@umontreal.ca

ABSTRACT:

Here we have rationally designed a tunable DNA-based nanoswitch whose closing/opening can be triggered over specific different pH windows. This nanoswitch forms an intramolecular triplex DNA structure through pH-sensitive parallel Hoogsteen interactions. We demonstrate that by simply changing the relative content of TAT/CGC triplets in the switch we can rationally tune its pH-dependence over more than 5 pH units. By using a combination of such nanowitches with different pH sensitivity, we also demonstrate how we can engineer a pH nanosensor that can precisely monitor pH variations over 5.5 units of pH. With their fast response time (<200 msec) and high reversibility, these pH-triggered nanoswitches appear particularly suitable for applications ranging from the real-time monitoring of pH changes in-vivo to the development of pH sensitive smart nanomaterial.

Nature often employs finely pH-regulated biomolecules to modulate and tune a number of biological activities[1] ranging from enzyme catalysis[2] to protein folding[3], membrane function[4] and apoptosis[5]. For these reasons, developing probes, switches or nanomaterials that are able to respond to specific pH changes should prove of utility for several applications in the fields of in-vivo imaging, clinical diagnostics, and drug-delivery[6-8].

By taking advantage of the high versatility and designability of DNA chemistry[9-19] several groups have recently developed pH-triggered DNA-based probes or nanomachines[20-30]. Such probes typically exploit DNA secondary structures that display pH-dependence due to the presence of specific protonation sites. These structures include I-motif [21-23,26,29,31], intermolecular triplex DNA[25,28,32], DNA tweezers[20] and, more recently, the A-motif[33]. Despite the promising and advantageous characteristics of some of these DNA-based nanomachines, which include fast response times and sustained efficiency over several cycles, a drawback inevitably affects their performances: they all respond (with an exception[33a]) over a fixed pH window that typically spans 1.5 to 2 pH units[26,34,33b]. These nanomachines, therefore, cannot be adapted to provide a useful output outside these fixed pH-windows.

Here we describe a method to rationally design and program pH-triggered DNA-based nanoswitches whose pH-dependence can be finely tuned and modulated over more than 5 units of pH. We created our switches by taking advantage of the well-characterized pH sensitivity of the parallel Hoogsteen (T,C)-motif in triplex DNA[34-36]. To do so we have designed a DNA-based triplex pH-triggered nanoswitch that consists in a double intramolecular hairpin stabilized with both Watson-Crick (W-C) and parallel Hoogsteen interactions (Fig. 1). More specifically, one hairpin of the triplex nanoswitch is formed by the W-C hybridization of two 10-base complementary portions separated by a 5 base loop. This duplex DNA is then able to form a triplex structure via the formation of a second hairpin through Hoogsteen parallel interactions with the other extremity of the switch (Fig. 1)[37]. Of note, while W-C base pairing is almost insensitive to pH[34], Hoogsteen interactions show a strong and variable pH-dependence [34-36]. More specifically, the CGC parallel triplet requires the protonation of the N3 of cytosine in the third strand in order to form (average pK_a of cytosines in triplex structure is ≈ 6.5 [35,38]) (Fig. 1, top). In contrast, the TAT triplets are relatively stable at neutral pH and are only destabilized at pH above 10 due to the deprotonation of thymine (pKa ~ 10)[39c] (Fig. 1, bottom). To follow opening/closing of the triplex portion of the switch, we labeled it with a fluorophore/quencher pair. More specifically, a fluorophore is conjugated at one end of the DNA sequence and a quencher is internally inserted in the loop of the hairpin duplex DNA so that the triplex-to-duplex transition (unfolding) brings the fluorophore away from the quencher and increases the fluorescence signal observed (Fig. 2). Of note, the fluorophore used in this work (AlexaFluor 680) is insensitive to pH over a wide pH window (Fig. S1)[40].

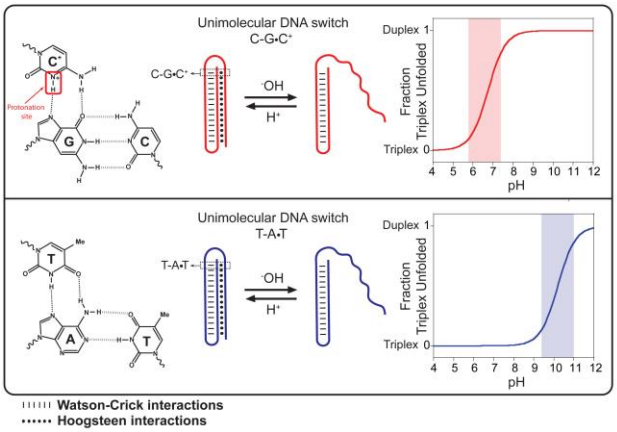

Figure 1. Here we designed programmable DNA-based triplex pH-triggered nanoswitches that form an intramolecular triplex structure through the formation of a Watson-Crick (dashed) pH-insensitive hairpin and a second Hoogsteen (dots) pH-sensitive hairpin. Because they require the protonation of the N3 of cytosine in the third strand (top, left), CGC triplets are only stable at acid pHs (average pK_a of cytosines in triplex structure is ≈ 6.5 [35]). For this reason, triplex switches containing only CGC triplets should unfold into an open duplex conformation at slightly acidic pHs. **Bottom**: In contrast, triplex switches containing only TAT triplets should unfold at much higher pHs due to deprotonation of thymine (pKa ~ 10)[39c].

Our DNA-based triplex nanoswitch is sensitive to pH. We first tested a switch containing an equal distribution of TAT and CGC triplets (50% TAT) (Fig. 2, orange curve). As expected, at very acidic pH values, the intramolecular double hairpin triplex structure is favored and we observe a very low fluorescence signal (fluorophore and quencher are brought in close proximity). As we increase the pH of the solution, the triplex structure is destabilized and we observe a gradual increase of the fluorescence signal characteristic of the triplex-to-duplex transition (unfolding). pH of semi-protonation (defined here as

pK_a^{obs}, the average pK_a due to several interacting protonation sites) for this triplex nanoswitch is 6.5.

We can tune the pH-dependence of our switches over a window of more than 5 units of pH by simply changing the relative content of CGC/TAT triplets in the sequence. For example, when the switch element contains only TAT triplets (100% TAT, *i.e.* no CGC triplets), the triplex-to-duplex transition occurs at basic pHs (pK_a^{obs} = 10.2) (Fig. 2, blue curve). By gradually replacing TAT triplets with CGC triplets, we can precisely program the switch so that it opens at a specific lower pH. By replacing 2 TAT triplets with 2 CGC triplets in the switch element's sequence, for example, we reduce the pK_a^{obs} of the switch from 10.2 to 8.6 (80% TAT, Fig. 2, dark green curve). The addition of four CGC triplets in the sequence further moves the pK_a^{obs} down to 7.5 (60% TAT, Fig. 2, light green curve). Finally, as shown above, a switch with an equal content of CGC vs TAT triplets shows a complete opening at slightly acidic pHs (pK_a^{obs}=6.5) (50% TAT, Fig. 2, orange curve). We note that triplex nanoswitches with higher CGC percentage content in the sequence (i.e. 40, 20 and 0% TAT) show the same pH-dependence of the one containing an equal content of CGC vs TAT (50% TAT) (Fig. S4).

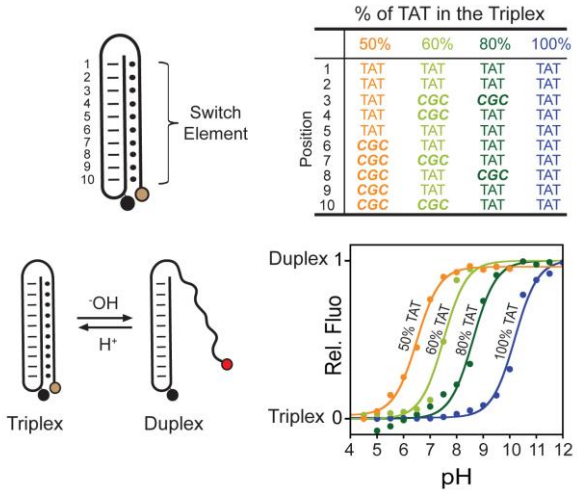

Figure 2. Top: Our triplex pH nanoswitches can be rationally programmed to be triggered over a specifically defined pH window. The pH sensitivity of the triplex interactions can be tuned by changing the CGC vs TAT content of the switch element, thus allowing to tune the pH window at which the triplex-to-duplex transition occurs (bottom, right). The opening of the switch containing only TAT triplets (100%TAT, blue curve), for example, is triggered at basic pHs (from 9 to 11), while the triplex structure of a switch with a 50% content of TAT (50% TAT, orange curve) is unfolded at a more acidic pH range (from 5 to 7). Switches with TAT contents between 50% and 100% show intermediate pH-sensitivity. Shown are the pH-titration curves (bottom, right) of the triplex nanoswitches (at 20 nM concentration) achieved in an universal citrate/phosphate/borate buffer[41] at 25°C. The triplex-to-duplex transition is monitored through a pH-insensitive fluorophore (AlexaFluor680) inserted at the 5'-end and a quencher (Black-Hole Quencher 2, BHQ-2) internally located in the switch. Of note, the Watson-Crick-stabilized hairpin remains folded over the wide range of pH investigated (Fig. S3).

The possibility to design triplex nanoswiches with tunable pH-dependence provides the opportunity to engineer pH sensors with unprecedented wide sensitivity to pH changes. As it is the case for most DNA-based pH-triggered nanodevices [26,33b,34], our programmable triplex nanoswitches show a limited and fixed dynamic range (defined here as the pH range at which the switches display 10% to 90% of their maximum signal) which spans approximately 1.9 units of pH (see, for example, 50% TAT, Fig. 3, left). This, in turn, corresponds to a change of $[H^+]$ concentration of 81-fold which represents the classic *dynamic range* window (the range of ligand concentration over which receptor occupancy shifts from 10% to 90%) inherent to single-site binding and Langmuir binding curves[42]. This fixed window can hinder the applicability of our switches where changes over a wider range of pH require to be monitored with precision. To overcome this problem we propose to extend this dynamic range by combining together two or more switches triggered over different pH windows[43]. For example, by combining together the 50%TAT and 80%TAT switches we created a pH sensor with a dynamic range that spans ~4.0 units of pH (from pH 5.5 to pH 9.5) (Fig. 3, center). A dynamic range of similar width, but shifted to more basic pHs (from pH 7.5 to pH 11.0), is also observed when combining the 80%TAT and 100%TAT switches (Fig. S5). Finally, by combining together three switches (50%, 80% and 100%TAT) we created a pH sensor displaying a dynamic range of ca. 5.5 units of pH (from pH 5.5 to pH 11.0).

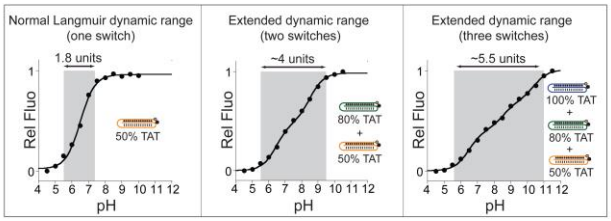

Figure 3. By combining together two or more switches we can create a pH-sensor displaying extended dynamic ranges. **Left:** A single switch shows a typical fixed dynamic range of ca. 1.9 units of pH (here the 50%TAT is only showed as example, see also Fig. 2). **Center**: By combining in the same solution two switches (i.e. 50%TAT and 80%TAT), each triggered over pH windows that are two orders of magnitude apart[43] (see Fig. 2), we can extend the useful dynamic range to ca. 4 units of pH. **Right**: It is possible to further extend the useful pH dynamic range (ca. 5.5 units of pH) by using together in the same solution three different switches (50%, 80% and 100%TAT). Shown are the pH-titration curves obtained using a universal citrate/phosphate/borate buffer and a total concentration of triplex nanoswitches of 20 nM (see SI for details).

Our switches respond to pH changes in milliseconds. We demonstrate this by performing stopped-flow experiments and by measuring the opening/closing reaction rates of each switch over its relevant pH dynamic range (Fig. 4, S6-S11). All switches show opening/closing kinetics (average time constant ~ 100 msec) sufficiently fast to allow the real time monitoring of pH variation in the millisecond range. Switches with a content of 20%, 60% and 80% TAT display measurable kinetics (see Fig. 4 and Table S1). In contrast, switches with a content of 0%, 50% and 100% TAT display kinetics so fast (< 3 msec) that their folding/unfolding transition's couldn't be determined using a conventional stopped-flow instrument.

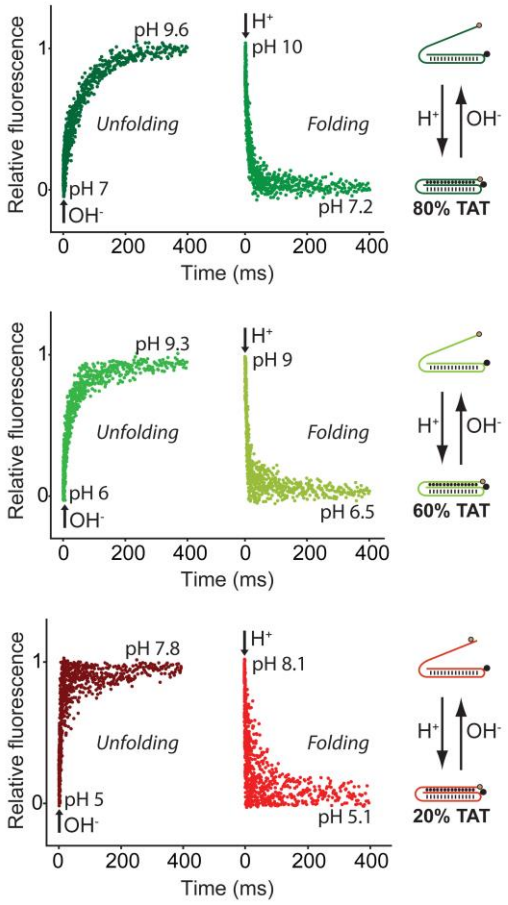

Figure 4. Our triplex pH nanoswitches respond to pH variation within milliseconds. For example, a switch containing 80% TAT triplets (top) displays an unfolding time constant ($t_{unfolding}$) of 61 ms and a folding time constant ($t_{folding}$) of 13 ms. Switches containing 60% of TAT (middle) and 20% of TAT (bottom) show even faster folding/unfolding rate constants (see table S1 for detailed rates). The experiments shown in this figure were performed by rapidly mixing (1:1) a buffered switch solution (final switch concentration = 100 nM) with a NaOH (0.015 M) or HCl (0.015 M) solution, to obtain a nearly 3-unit pH change (see SI). Each kinetic trace shown is an average of 10 acquisitions.

The switches are reversible and only respond over a specific pH window. To demonstrate this we selected three switches that are triggered over three different pH windows (20%, 60% and 100%TAT, see Fig. 2 and Fig. S2) and tested them with a series of cyclic pH-jump experiments (Fig. 5). In the first experiment, for example, the pH of the three solutions containing the switches (each solution containing a different switch) was cycled from pH 5.0 to pH 7.0 and back to pH 5.0 for five times (see Fig. 5, top). Only the 20%TAT switch was triggered over this pH window while the other two switches (60% and 100%TAT) did not give any significant signal change. In the other two series of experiments (Fig. 5, center and bottom) we selected different pH-jumps to trigger only one switch. In all three experiments we observed a high reversibility of the switches' signal and a minimal cross-activation coming from the other two switches. A similar experiment was carried out with these same switches but, this time, by mixing them in equimolar amount in the same solution. The pH of the solution was cyclically changed to unfold/fold only one switch at a time (Fig. S12). As expected, the fluorescence change observed was consistent with the opening /closing of a single switch thus further demonstrating both the reversibility and specificity of our triplex nanoswitches.

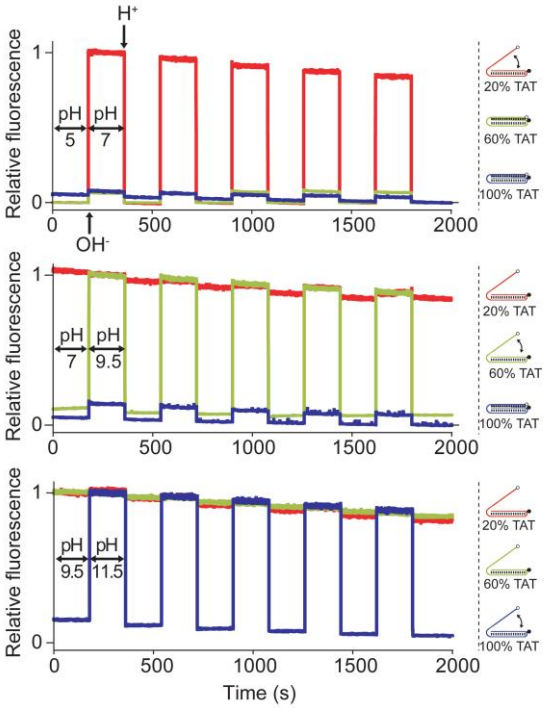

Figure 5. Our triplex pH nanoswitches show high reversibility and no cross-activation. This is demonstrated by cyclically changing the pH of three solutions each containing a single switch (20%, 60% and 100%TAT). **Top**: Cycling the pH from 5.0 to 7.0 (and *viceversa*) only activates the most unstable switch (20% TAT, red line) while no significant signal is observed for the switches with higher TAT content (60%TAT, 100%TAT). **Center**: A pH change from 7.0 to 9.5 leads to opening/closing of only the 60%TAT switch (green line). Within this pH window the 100%TAT switch (blue line) remains closed while the 20% TAT switch is already completely open. **Bottom:** When the pH solution is cycled between 9.5 and 11.5 we observe the opening/closing transition of the 100%TAT (blue line) while the other two switches are already completely open within this pH range. Each solution contains only one switch (20 nM) and the pH of the solution was cyclically changed by adding small aliquots of NaOH or HCl. We note that the small drift of fluorescence signal observed over time is likely due to the increase of the ionic strength of the solution upon NaOH or HCl additions.

Here we have rationally designed a DNA-based triplex nanoswitch with tunable pH-dependence. The nanoswitch forms an intramolecular triplex DNA structure and takes advantage of the different pH-dependence of TAT and CGC Hoogsteen interactions (triplets). By rationally changing the relative content of TAT/CGC triplets in the switch we demonstrate for the first time that we can precisely tune its pH-dependence over more than 5 units of pH. For example, a switch with a high CGC content (≥50%) is triggered near a pH of ~5.5-6.0 while a switch with lower CGC content (<50%) is triggered at gradually more basic pHs. The tunability of such pH-triggered switch represents an unprecedented advantage. For example, this allows to program switches for various specific applications that might require the opening/closing of the switch over different pH windows. Also, the capacity to tune the pH-dependence with great precision offers the possibility to extend the range of pH at

which we can observe the opening/closing of the switch. We demonstrate this by mixing and matching switches of different pH-dependence. Using this strategy, we have developed a fluorescent pH-nanometer displaying an unprecedented wide pH window of 5.5 units over which the sensor responds linearly. In addition of being programmable, our triplex DNA-switch also displays much faster dynamics than other examples reported in the literature. Because most of the pH-controlled DNA switches are currently based on the association/dissociation of two different strands[33] or on the conformation switch of constrained structures[8,26], their folding (or unfolding) kinetic remains typically quite slow (i.e. seconds[8, 26, 33b] or min[20]). In contrast, the structure-switching mechanism of our switch occurs through a fast intramolecular opening/closing transition with a response time below 100 msec. This feature has important implications for imaging[8,18c,26] and drug-release applications that require the real-time simultaneous activation of the switch upon pH changes.

Because pH dysregulation is an hallmark of cancer and many cancers are characterized by an inverted pH gradient between the inside and the outside of cells[44], our switches could be of value for diagnostic purposes. Finally, the ability to program DNA strands to open/close over a specific pH window could find many applications in the field of DNA nanomachines[45], drug delivery systems[46] and smart nanomaterials[47].

ACKNOWLEDGEMENTS

This work was supported by the MIUR (FIRB "Futuro in Ricerca") (FR), by Bill & Melinda Gates Foundation through the Grand Challenges Explorations (OPP1061203) (FR), by the International Research Staff Exchange Scheme (IRSES) grant under the Marie Curie Actions program (FR) and by the National Sciences and Engineering Research Council of Canada through Grant No. 436381-2013(NSERC) (AVB). FR is supported by a Marie Curie Outgoing Fellowship (IOF) (Proposal 298491 under FP7-PEOPLE-2011-IOF), AI is supported by Canada-Italy Innovation Award 2013, AVB is a fellow of le Fond de Recherche Santé du Québec.

SUPPORTING INFORMATION AVAILABLE

Supporting methods, figures. This material is available free of charge at http://pubs.acs.org.

REFERENCES

1) a) Frantz, C.; Barreiro, G.; Dominguez, L.; Chen, X.; Eddy, R.; Condeelis, J.; Kelly, J. S. M.; Matthew P. Jacobson, M. P.; Barber, D. L. *J. Cell Biol.* **2008**, *183*, 865–879. b) Lukin, J. A. *Chem. Rev.* **2004**, *104*, 1219–1230. c) McLachlan, G. D.; Cahill, S. M.; Girvin, M. E.; Almo, S. C. *Biochemistry* **2007**, *46*, 6931–6943.

2) a) Nishi, T.; Forgac, M. *Nature Rev. Mol. Cell Biol.* **2002**, *3*, *94-103*; b) Slepkov, E. R.; Rainey, J. K.; Sykes, B. D.; Fliegel, L. *Biochem. J.* **2007**, *401*, *623–633*.

3) a) Lagadic-Gossmann, D.; Huc, L.; Lecureur, V. *Cell Death Differ.* **2004**, *11*, 953–961. b) Matsuyama, S.; Llopis, J.; Deveraux, Q.L.; Tsien, R.Y.; Reed, J.C. *Nat. Cell. Biol.* **2000**, *2*, 318–325.

4) a) Paroutis, P.; Touret, N.; Grinstein, S. *Physiology* **2004**, *19*, *207–215*. b) Busa, W. B.; Nuccitelli, R. *Am. J. Physiol.* **1984**, *246*, R409-438.

5) a) Gorfe, A. A.; Caflisch A. *Structure* **2005**, *13*, 1487–1498. b) Morikis, D.; Elcock, A. H.; Jennings, P. A.; McCammon, J. A. *Protein Sci.* **2001**, *10*, 2379–2392. c) Tews, I.; Findeisen, F.; Sinning, I.; Schultz, A.; Schultz, J. E.; Linder, J. U. *Science* **2005**, *308*, 1020–1023.

6) a) Abbaspourrad, A.; Datta, S. S.; Weitz, D. A. *Langmuir* **2013**, *29*, 12697−12702. Leblond, J.; Gao, H.; Petitjean, A.; Leroux, J.C. *J. Am. Chem. Soc.* **2010**, *132*, 8544–8545. b) Convertine, A. J.; Diab, C.; Prieve, M.; Paschal, A.; Hoffman, A. S.; Johnson, P. H.; Stayton, P. S. *Biomacromolecules* **2010**, *11*, 2904–2911. c) Wu, X. L.; Kim, J. H.; Koo, H.; Bae, S. M.; Shin, H.; Kim, M. S.; Lee, B. H.; Park, R.; Kim, I.; Choi, K.; Kwon, I. C.; Kim, K.; Lee, D. S. *Bioconjugate Chem.* **2010**, *21*, 208–213. d) Zhou, K.; Liu, H.; Zhang, S.; Huang, X.; Wang, Y.; Huang, G.; Sumer, B.D.; Gao, J. *J. Am. Chem. Soc.* **2012**, *134*, 7803−7811.

7) a) Chan, K. W. Y.; Liu, G.; Song, X.; Kim, H.; Yu, T.; Arifin, D. R.; Gilad, A. A.; Hanes, J.; Walczak, P.; van Zijl, C. M.; Bulte, J. W. M.; McMahon, M. T. *Nature Materials* **2013**, *12*, 268-275. b) Gallagher, F. A.; Kettunen, M. I.; Day, S. E.; Hu, D. E.; Ardenkjær-Larsen, J. H.; Zandt, R.; Jensen, P. R.; Karlsson, M.; Golman, K.; Lerche, M. H.; Brindle, K. M. *Nature* **2008**, *453*, 940-944. c) Urano, Y.; Asanuma, D.; Hama, Y.; Koyama, Y.; Barrett, T.; Kamiya, M.; Nagano, T.; Watanabe, T.; Hasegawa, A.; Choyke, P. L.; Kobayashi, H. *Nat. Med.* **2009**, *15*, 104-109.

8) Modi, S.; Nizak, C.; Surana, S.; Halder, S.; Krishnan, Y. *Nat. Nanotechnol.* **2013**, *8*, 459–467.

9) Bath, J.; Tuberfield, A. J. *Nat. Nanotech.* **2007**, *2*, *275-284.*

10) Seeman, N. C. *Annu. Rev. Biochem.* **2010**, *79*, *65–87*.

11) Dittmer, W. U.; Reuter, A.; Simmel, F. C. *Angew. Chem. Int. Ed.* **2004**, *43*, 3550 –3553.

12) Wieland, M.; Benz, A.; Haar, J.; Halder, K.; Hartig, J. S. *Chem. Commun.* **2010**, *46*, 1866–1868.

13) Zhou, C.; Yang, Z.; Liu, D. *J. Am. Chem. Soc.* **2012**, *134*, 1416−1418.

14) Thomas, J. M.; Yu, H. Z.; Sen, D. *J. Am. Chem. Soc.* **2012**, *134*, 13738−13748.

15) Li, X. M.; Li, W.; Ge, A. Q.; Chen, H. Y. *J. Phys. Chem. C* **2010**, *114*, 21948–21952.

16) McLaughlin, C.K.; Hamblin, G.D.; Sleiman, H.F. *Chem. Soc. Rev.* **2011**, *40*, 5647–5656.

17) a) Seelig, G.; Soloveichik, D.; Zhang, D. Y.; Winfree, E. *Science* **2006**, *314*, 1585-1588. b) Teller, C.; Willner, I. *Curr. Op. Biotechn.* **2010**, *21*, 376–391. c) Andersen, E. S.; Dong, M.; Nielsen, M. M.; Jahn, K.; Subramani, R.; Mamdouh, W. et al., *Nature* **2009**, *459*, 73-76. d) Keefe, A. D.; Pai, S.; Ellington, A. *Nature Reviews Drug Discovery*, **2010**, *9*, 537-550. e) Zhang, D.Y.; Winfree E. *J. Am. Chem. Soc*. **2008**, *130*, 13921-13926. f) McLaughlin, C.K.; Hamblin, G.D.; Haenni, K.; Conway, J.W.; Nayak, M.K.; Carneiro, K.M.M.; Bazzi, H.S.; Sleiman, H.F. *J. Am Chem. Soc.* **2012**, *134*, 4280-4283. g) Greschner, A.; Bujold, K.; Sleiman H.F. *J. Am. Chem. Soc.*, **2013**, *135*, 11283-11286.

18) a) Simmel, F. C. *Angew. Chem. Int. Ed*. **2008**, *47*, 5884-5887. b) Krishnan, Y.; Simmel, F. C. *Angew. Chem. Int. Ed.* **2011**, *50*, 3124-3156. c) Bhatia, D.; Sharma, S.; Krishnan, Y. *Curr Opin Biotechnol*, **2011**, *22*, 475-484.

19) Vallée-Bélisle, A.; Ricci, F.; Plaxco, K. W. *Proc. Natl. Acad. Sci. USA.* **2009**, *106*, 13802-13807.

20) a) Shimron, S.; Magen, N.; Elbaz, J.; Willner, I. *Chem. Commun.* **2011**, *47*, 8787–8789. b) Elbaz, J.; Want, Z.G.; Orbach, R.; Willner, I. *Nano Lett.* **2009**, *9*, 4510–4514. c) Wang, Z.G.; Elbaza, J.; Remacle, F.; Levinea,

R. D.; Willner, I. *Proc. Natl. Acad. Sci. USA.* **2010**, *107*, 21996-22001.
21) Li, T.; Famulok, M. *J. Am. Chem. Soc.* **2013**, *135*, 1593−1599.
22) Liu, D.; Balasubramanian, S. *Angew. Chem. Int. Ed.* **2003**, *115*, 5912 –5914.
23) Liu, D.; Bruckbauer, A.; Abell, C.; Balasubramanian, S.; Kang, D.; Klenerman, D.; Zhou, D. *J. Am. Chem. Soc.* **2006**, *128*, 2067−2071.
24) Zhou, J.; Amrane, S.; Korkut, D. N.; Bourdoncle, A.; He, H. Z.; Ma, D. L.; Mergny, J. L. *Angew. Chem. Int. Ed*. **2013**, *52*, 7742 –7746.
25) Brucale, M.; Zuccheri, G.; Samorì, B. *Org. Biomol. Chem.* **2005**, *3*, 575-577.
26) Modi, S.; Swetha, M. G.; Goswami, D.; Gupta, G. D.; Mayor, S.; Krishnan, Y. *Nat. Nanotechnol.* **2009**, *4*, 325-330.
27) Chen, L.; Di, J.; Cao, C.; Zhao, Y.; Ma, Y.; Luo, J.; Wen, Y.; Song, W.; Songd, Y.; Jiang, L. *Chem. Commun.* **2011**, *47*, 2850-2852.
28) Chen, Y.; Lee, S-H; Mao, C. *Angew. Chem. Int. Ed.* **2004**, *43*, 5335-5338.
29) Wang, W.; Yang, Y.; Cheng, E.; Zhao, M.; Meng, H.; Liu, D.; Zhou, D. *Chem. Commun.* **2009**, *7*, 824-826.
30) Liedl, T.; Simmel, F.C. *Nano Letters* **2005**, 5, 1894-1898.
31) Liu, H.; Xu, Y.; Li, F.; Yang, Y.; Wang, W.; Song, Y., Liu, D. *Angew. Chem. Int. Ed.* **2007**, 46, 2515-2517.
32) a) Han, X.; Zhou, Z.; Yang, F.; Deng, Z. *J. Am. Chem. Soc.* **2008**, *130*, 14414-14415. b) Kolaric, B.; Sliwa, M.; Brucale, M.; Vallée, R. A. L.; Zuccheri, G.; Samori, B.; Hofkensa, J.; De Schryver, F. C. *Photochem. Photobiol. Sci.* **2007**, *6*, 614–618. c) Li, X.M.; Song, J.; Cheng, T., Fu, P.Y., *Anal. Bioanal. Chem.* **2013**, *405*, 5993–5999.
33) a) Saha, S.; Chakraborty, K.; Krishnan, Y. *Chem. Comm.* **2012**, *48*, 2513-2515. b) Chakraborty, K.; Sharma, S.; Maiti, P. K.; Krishnan, Y. *Nucl. Acid Res.* **2009**, *97*, 2810-2817.
34) Ohmichi, T.; Kawamoto, Y.; Wu, P.; Miyoshi, D.; Karimata, H.; Sugimoto, N. *Biochemistry* **2005**, *44*, 7125-7130.
35) Leitner, D.; Schröder, W.; Weisz, K. *Biochemistry* **2000**, *39*, 5886-5892.
36) Sugimoto, N.; Wu, P.; Hara, H.; Kawamoto, Y. *Biochemistry* **2001**, *40*, 9396-9405.
37) a) Sklenar, V.; Feigon, J. *Nature* **1990**, *345*, 836-838; b) Haner, R.; Dervan, P. B. *Biochemistry* **1990**, *29*, 9761-9765. b) Volker, J.; Botes, D. P.; Lindsey, G. G.; Klump, H. H. *J. Mol. Biol.* **1993**, *230*, 1278-1290.
38) a) Asensio, J. S.; Lane, A. N.; Dhesi, J.; Bergqvist, S.; Brown, T. *J. Mol. Biol.* **1998**, *275*, 811-822. b) Husler, P. L.; Klump, H. H. *Archieved of biochemistry and biophysics* **1995**, *317*, 46-56.
39) Liu, Z.; Li, Y.; Tian, C.; Mao, C. *Biomacromolecules* **2013**, *14*, 1711-1714. b) Keppler, M. D.; Fox, K. R. *Nucl. Acid Res.* **1997**, *25*, 4644-4649. c) W. Saenger, in: Ch.R. Cantor (Ed.), Principles of Nucleic Acid Structure, Springer, New York, 1984.
40) Panchuk–Voloshina, N.; Haugland, R. P.; Bishop–Stewart, J.; Bhalgat, M. K.; Millard, P. J.; Mao, F.; Leung, W. Y.; Haugland, R. P. *J. Histochem. Cytochem.* **1999**, *47*, 1179-1188.
41) Östling, S.; Virtama, P. *Acta Phys. Scandinav.* **1946**, *11*, *289-293*.
42) a) Ferrell, J. E. Jr. *Trends Biochem. Sci.* **1996**, *21*, *460*. b) Goldbeter, A.; Koshland, D. E. Jr. *Q. Rev. Biophys.* **1982**, *15*, 555-591.
43) a) Vallée-Bélisle, A.; Ricci, F.; Plaxco, K. W. *J. Am. Chem. Soc.* **2012**, *134*, 2876-2879. b) Porchetta, A.; Vallée-Bélisle, A.; Plaxco, K. W.; Ricci, F. *J. Am. Chem. Soc.* **2012**, *134*, 20601-20604.
44) a) Webb, B. A.; Chimenti, M.; Jacobson, M. P.; Barber, L. P. *Nature Reviews* **2011**, *11*, 671-677. b) Gerweck, L.E.; Seetharaman, K. *Cancer Res.* **1996**, *56*, 1194-1198.
45) a) Turberfield, J.; Mitchell, J.C.; Yurke, B.; Mills, A.P.; Blakey, M.I.; Simmel, F.C. *Phys. Rev. Lett.* **2003**, *90*, 118102-118105. b) Simmel, F.C. *Nanomedicine* **2007**, *2*, 817-830.
46) a) Ahmed, F.; Pakunlu, R.I.; Srinivas, G.; Brannan, A.; Bates, F.; Klein, M.L.; et al. *Mol. Pharm.* **2006**, *3*, 340-350. b) Bae, Y.; Fukushima, S.; Harada, A.; Kataoka, K. *Angew. Chem. Int. Ed.* **2003**, *42*, 4640-4643.
47) a) Su, J.; Chen, F.; Cryns, V. L.; Messersmith, P. B. *J. Am. Chem. Soc.* **2012**, *133*, 11850–11853. b) Tian, J.; Ding, L.; Xu, H.; Shen, Z.; Ju, H.; Jia, L.; et al. *J. Am. Chem. Soc.* **2013**, *135*, 18850-18858. c) Du, J.; Du, X.; Mao, C.; Wang, J. *J. Am. Chem. Soc.* **2011**, *133*, 17560-17563.

TOC Graphic

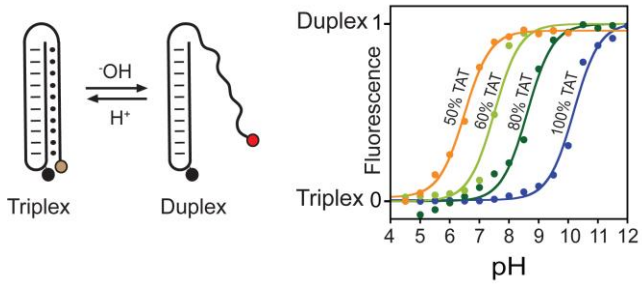
Triplex
Duplex
$^{-}$OH
H^{+}
Duplex 1
Triplex 0
Fluorescence
50% TAT
60% TAT
80% TAT
100% TAT
4 5 6 7 8 9 10 11 12
pH